Phase Behavior of Elastin-Like Synthetic Recombinamers in Deep Eutectic Solvents

ARTICLE *in* BIOMACROMOLECULES · MAY 2012

Impact Factor: 5.75 · DOI: 10.1021/bm300200e · Source: PubMed

Article

pubs.acs.org/Biomac

Phase Behavior of Elastin-Like Synthetic Recombinamers in Deep Eutectic Solvents

Stefania Nardecchia,[†] María C. Gutiérrez,[†] M. Luisa Ferrer,[†] Matilde Alonso,[‡] Isabel M. López,[‡] J. Carlos Rodríguez-Cabello,[‡] and Francisco del Monte*[,†]

[†]Instituto de Ciencia de Materiales de Madrid (ICMM), Consejo Superior de Investigaciones Científicas (CSIC), Cantoblanco 28049, Madrid, Spain

[‡]GIR Bioforge, University of Valladolid, 47011 Valladolid, Spain

ABSTRACT: Deep eutectic solvents promoted the stabilization of the collapsed state of elastin-like recombinamers − and the subsequent formation of aggregates − upon the loss of the structural water molecules involved in hydrophobic hydration. Cryo-etch scanning electron microscopy allowed the observation of these aggregates in neat deep eutectic solvents. The suppression of the lower critical solution temperature transition, observed by differential scanning calorimetry and dynamic light scattering, confirmed the presence of the elastin-like recombinamers in their collapsed state. Actually, the transition from the collapsed to the expanded state was suppressed even after moderate aqueous dilution − for water contents ranging from nil to ca. 45 wt % − and it was only recovered upon further addition of water − above 50 wt %. These features revealed the preferred stabilization of the collapsed state in not only neat deep eutectic solvents but also partially hydrated deep eutectic solvents. We consider that the capability to trigger the lower critical solution temperature transition by partial hydration of deep eutectic solvent may open interesting perspectives for nano(bio)technological applications of elastin-like recombinamers.

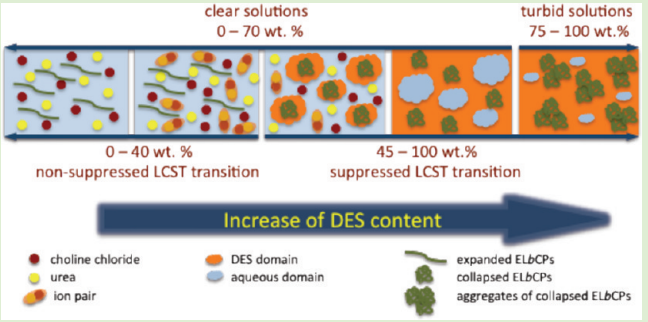

INTRODUCTION

Elastin-like polymers (ELPs) are synthetic polypeptides whose composition has been inspired by the repeating sequences found in natural elastin.[1−8] Poly(VPGVG) is one of the most important member of the elastin-like family,[9] where G stands for glycine, V stands for L-valine, and P stands for L-proline. Derivatives can be obtained by systematic substitutions of the valine amino acid residues of the pentamer by either natural or non-natural L-amino acids. In any case, the polymer chain is predominantly a hydrophobic polypeptide, where the only polar groups are the peptide-bond moieties themselves.[10]

In aqueous solutions, ELPs exhibit the capability to undergo a lower critical solution temperature (LCST) transition from a random coil to a collapsed (e.g., globular-like) structure mimicking the transition between the unfolded to the folded structure of natural elastins.[11−13] It is widely accepted that in the collapsed state the polymer chains adopt a dynamic, regular, nonrandom structure stabilized by hydrophobic contacts that ultimately results in a phase-separated state.[2,14−17] Mechanisms based on transition from expanded to collapsed state are actually behind the stimuli-responsive features of PNIPAM (poly(isopropyl acrylamide)), one of the most well-known thermoresponsive synthetic polymers that is often used as simple model for proteins.[18]

Nowadays, recombinant technology allows the production of special ELPs (the so-called elastin-like recombinamers - ELRs) with a precision, monodisperse nature and degree of complexity that is not comparable to their chemically synthesized counterparts (e.g., bare ELPs).[19] Interestingly, tailored molecular designs of ELRs allow switching the loss of hydrophobic hydration water that characterizes the LCST transition from the expanded to the collapsed state in response to different stimuli (e.g., not only different temperatures but also, under isothermal conditions, changes in pH or light).[2] This feature offers a tremendous versatility as compared with other synthetic stimuli-responsive polymers. For instance, dual-stimuli-responding polymers can be obtained from block copolymers (e.g., poly(*N*-isopropyl acrylamide-*co*-acrylic acid)) in which one component is temperature-sensitive and the other one is pH-sensitive (*N*-isopropyl acrylamide and acrylic acid, respectively).[20]

Taking into account the fact that the LCST transition is related to hydrophobic association, one may wonder whether the transition from the random coil to the globular-like structure of ELRs takes place in nonaqueous solvents. This question might lack of interest for regular organic solvents if one considers that some of the most typical applications of ELRs are in biomedicine and biotechnology in which toxicity

Received: February 6, 2012
Revised: May 23, 2012
Published: May 25, 2012

issues play a capital role.[21,22] However, deep eutectic solvents (DESs)[23] are lately offering an interesting alternative to regular organic solvents for number of applications. DESs are obtained by complexion of quaternary ammonium salts with hydrogen bond donors. The charge delocalization occurring through hydrogen bonding between the halide anion with the hydrogen-donor moiety is responsible for the decrease in the freezing point of the mixture relative to the melting points of the individual components. DESs have been used as suitable solvents for dissolution/dispersion of number of biological entities (ranging from biomolecules up to microorganisms)[24−28] and biopolymers[29−31] but never for ELRs.

Herein, we have studied the dissolution/dispersion of ELRs in DES. The DES of choice was based on a mixture of urea and choline chloride in a 2:1 molar ratio (UCCl-DES). Since the seminal work by Abbot and coworkers describing a set of different DESs,[23] UCCl-DES has become one the most widely studied DESs and can be considered to be a model system. Actually, it has been the mixture of choice in number of papers studying the dissolution of biomolecules and biopolymers.[24−31] With regards to ELRs, we used a linear diblock AB architecture (EL*2b*R) and a linear tetrablock $(AB)_2$ architecture (EL*4b*R). In both cases, one of the blocks consisted of a poly(L-valine−L-proline−L-glycine−L-valine−L-glycine) (VPGVG) in which the second valine has been regularly replaced by an L-glutamic acid (E) in one pentapeptide out of five, whereas the second block was a poly(L-valine−L-proline−L-alanine−L-valine−L-glycine) (VPAVG) in the diblock architecture and a poly(L-valine−L-glycine−L-isoleucine−L-proline−L-glycine) (VGIPG, where I stands for L-isoleucine) in the tetrablock one.[32,33] Therefore, the polypeptide architecture of EL*2b*R was $[(VPGVG)_2(VPGEG)(VPGVG)_2]_{20}$-$(VPAVG)_{40}$ (M_W = 58.5 KDa), whereas that of EL*4b*R was $\{[(VPGVG)_2$-$(VPGEG)$-$(VPGVG)_2]_{10}$-$[VGIPG]_{60}\}_2$ (M_W = 92.9 KDa). Both recombinamers can be considered to be simple stimuli-responsive polymers showing temperature and pH sensitiveness due to the presence of the glutamic acid residues. In practical terms, the apparent complexity of their respective block architecture just determines the temperature at which the LCST transition occurs (e.g., 33 °C for EL*2b*R and 16 °C for EL*4b*R).[32,33] The LCST transition of elastin-like block-recombinamers (EL*b*Rs) in UCCl-DES and aqueous dilutions of DES was studied by differential scanning calorimetry (DSC) and dynamic light scattering (DLS). The occurrence of EL*b*R phase segregation and aggregation in UCCl-DES was studied by cryo-etch-SEM.

EXPERIMENTAL PART

The preparation of UCCl-DES was accomplished by heating urea (from Aldrich) and choline chloride (from Aldrich) in a 2:1 molar ratio at 80 °C and stirring until a homogeneous liquid was formed.

The preparation of EL*b*Rs was accomplished as described elsewhere.[32] In brief, synthetic DNA duplexes encoding the oligopeptide $(VPGVG)_2$-(VPGEG)-$(VPGVG)_2$ and the oligopeptide $(VPAVG)_{20}$ (or $(VGIPG)_{60}$) were generated by polymerase chain reaction (PCR) amplification using synthetic oligonucleotides. The gene cloning, concatenation, and colony screening were performed as previously described.[34] Selected genes were subcloned into a modified pET-25(b) expression vector and transformed into the *E. coli* strain BLR(DE3). Expression conditions and purification protocols were as previously described.[34] Production yields for all of the polymers were between 80 and 200 mg/mL of bacterial culture.

The incorporation of EL*b*Rs in UCCl-DES was accomplished by (1) dissolution of EL*b*R in water (1 or 5 wt %, under stirring over 24 h at 4 °C), (2) dissolution of the components that form the DES (e.g., urea and choline chloride in a 2:1 molar ratio) in the aqueous solution of EL*b*R (under stirring over further 24 h at 4 °C), and (3) freeze-drying.

Cryo-etch-SEM experiments were carried out on aqueous solutions of UCCl-DES, of EL*b*R and of UCCl-DES also containing EL*b*R. The aqueous solution of UCCl-DES was prepared by simple dissolution of the DES components in water. The UCCl-DES content in solution ranged from 0.6 to 1 wt %. The aqueous solutions of EL*b*R (without DES) were prepared under stirring over 24 h at 4 °C and then stored over another 24 h before analysis. The EL*b*R content in solution was always 2.5 wt %. The preparation of the aqueous solutions of UCCl-DES with EL*b*R was accomplished upon the addition of the DES components (urea and choline chloride in a 2:1 molar ratio and in the wt % mentioned above) to the aqueous solutions of EL*b*R described above. The solutions (any) were always stirred over 24 h at 4 °C and then stored at the same temperature over further 24 h before analysis. For comparison, aqueous solutions of EL*b*R (without UCCl-DES) that also contain NaCl (100 mM) were also studied. The aqueous solutions were placed in the sample holder of a cryotransfer system (Oxford CT1500), plunged into subcooled liquid nitrogen, and then transferred to a preparation unit via an air lock transfer device. The frozen specimens were cryofractured and transferred directly via a second air lock to the microscope cold stage, where they were etched for 2 min at −90 °C. After ice sublimation and in the preparation unit, the etched surfaces were sputter-coated with gold for 10 min at a sputter current of 10 mV. The thickness of the resulting gold film was within the 5−10 nm range, which allows for the undistorted observation of EL*b*R aggregates of ca. 100 nm diameter. Samples were subsequently transferred onto the cold stage of the scanning electron microscope chamber. Fractured surfaces were observed with a DSM 960 Zeiss scanning electron microscope at −135 °C under the following conditions: acceleration potential, 15 kV; working distance, 15 mm; and probe current, 5−10 nA.

DSC scans were carried out on aqueous solutions of EL*b*R (1 and 5 wt %) without and with UCCl-DES using a Mettler Toledo 822 DSC equipped with a liquid-nitrogen cooler and calibrated with a standard sample of indium. The aqueous solutions of EL*b*R without UCCl-DES were prepared under stirring over 24 h at 4 °C and then stored at 25 °C over another 24 h before analysis. The preparation of the aqueous solutions EL*b*R with DES was accomplished upon the addition of the DES components (urea and choline chloride in a 2:1 molar ratio) right after the addition of the aqueous solutions of EL*b*R; the solution was stirred over 24 h at 4 °C and then was stored at 25 °C over another 24 h. The final UCCl-DES content (in wt %) in the aqueous solutions EL*b*R was simply determined by the mass of urea and choline chloride added to the solution. After this period, 20 μL of any of these solutions (e.g., with or without UCCl-DES) was placed in 40 μL of aluminum pans hermetically sealed. An equal volume of water was placed in the reference pan. The heating program consisted of an initial isothermal stage (5 min at 5 °C), followed by heating at a constant rate of 5 °C min^{-1} from 0 to 60 °C and cooling at −5 °C min^{-1} to 0 °C.

DLS analyses were carried out on aqueous solutions of EL*b*R (1 wt %) that also contained UCCl-DES (45 and 55 wt %) using a Zetasizer Nano S (Malvern Instruments) equipped with a Peltier temperature controller. The aqueous solutions of EL*b*R either without or with UCCl-DES were prepared as described above for DSC experiments. After preparation, 400 μL of these solutions was placed into a PMMA cuvette. Data were collected within the 0 − 50 °C interval using a 1 °C min^{-1} heating ramp. The stabilization time between measurements was 10 min. The experiments were carried by quintuplicate.

RESULTS AND DISCUSSION

Both EL*2b*R and EL*4b*R were readily soluble in cold water (at temperatures below the LCST) but not in neat UCCl-DES. Therefore, direct addition of any of the EL*b*Rs to neat UCCl-DES resulted in a nonhomogeneous suspension that resembled those obtained upon direct addition of any ELP to water when the temperature is above its respective LCST. Actually, the viscosity of UCCl-DES made any attempt for EL*b*Rs

homogenization even more difficult than in water. Under these circumstances, the incorporation of EL*b*Rs in UCCl-DES was accomplished following an indirect procedure that allows transitioning from aqueous to DES chemistry.[35] In brief, the procedure consisted of (1) dissolution of EL*b*R in water (1 wt %, under stirring over 24 h at 4 °C), (2) dissolution of the components that form the DES (e.g., urea and choline chloride) in the EL*b*R aqueous solution (under stirring over further 24 h at 25 °C), and (3) freeze-drying. The concentration of urea and choline chloride added in (2) was so chosen for a final EL*b*R content in UCCl-DES that ranged from 1 to 5 wt %. After freeze-drying, the turbid-like nature of the resulting UCCl-DES suspensions of EL*b*Rs (Figure 1) was indicative of the formation of aggregates, the size of which was large enough to scatter visible wavelengths.

Figure 1. Left: clear solution resulting from EL*2b*R dissolution in water at 4 °C. Right: turbid suspension of EL*2b*R in DES (prepared as described in the main text). The EL*2b*R content was 1 wt % in both cases.

The turbidity of UCCl-DES suspensions of EL*b*Rs resembled that of EL*b*Rs in aqueous solutions above the LCST.[32,33] In this latter case, the free polymer chains of EL*b*Rs that remained disordered (e.g., in form of fully hydrated − by hydrophobic hydration − random coils) below the LCST undergo a hydrophobically driven collapse and assemble into a phase-separated state above the LCST. According to Urry's and Tamburro's models,[14−17] the polymer chains adopt a dynamic, regular, nonrandom structure, called a β-spiral, that involves type II β-turns as the main secondary structural feature and is stabilized by intraspiral interturn and interspiral hydrophobic contacts. When the concentration of EL*b*R in aqueous solution is above a threshold value, hydrophobic contacts can be established not only between segments of an individual polymer chain - to form single globules - but also between segments of two or more different polymer chains and then form globular aggregates that scatter visible wavelengths.[36] Eventually, turbid gels are typically obtained when these aggregates are capable of forming a continuous network across the entire original solution.[33] In neat UCCl-DES, we hypothesized that the absence of water promotes EL*b*Rs to lose essentially all of the ordered water structures resulting from hydrophobic hydration and hence the formation of globular aggregates.

The occurrence of EL*b*R phase segregation (to the collapsed state) and aggregation (of the resulting globules) upon freeze-drying was first studied by cryo-etch-SEM. In cryo-etch-SEM experiments, aqueous samples are plunge-frozen by immersion in subcooled liquid nitrogen (e.g., liquid nitrogen at vacuum pressure). Under these circumstances, the freezing rate is $\sim 10^4$ °C s^{-1}.[37] This freezing rate is far from that needed to obtain supercooled water by freezing of pure water solutions (ca. 10^6 °C s^{-1}).[38] However, the presence of impurities makes freezing rates of $\sim 10^4$ °C s^{-1} fast enough to impede the formation of crystalline ice.[37] The frozen specimens were cryo-fractured and transferred to the microscope cold stage, where the temperature is subsequently raised to −90 °C to favor the formation of crystalline ice that, in pseudodiluted samples, readily frees itself of any solute and concentrates between adjacent ice crystals. Exposed ice vaporizes by sublimation in an etching-like process so that the resulting morphology corresponds to empty areas (where ice originally resided) surrounded by the concentrated solutes in a "fence-like" fashion. In summary, cryo-etch-SEM allows the observation of any solute originally dissolved in water after the submission of this solution to a freeze-drying process. This is why we considered that cryo-etch-SEM was a suitable technique for the observation of EL*b*R aggregates in UCCl-DES. Actually, cryo-etch-SEM has been previously used for observation of either the expanded or the collapsed state of EL*b*R upon the freezing of aqueous solutions (without further additives) that, respectively, were below or above the phase transition.[39,40] Nonetheless, it is worth noting that the formation of "fence-like" morphologies is mainly governed by the cryo-etch process and neither the composition nor the conformation of the solutes play a capital role in this issue. Actually, "fence-like" morphologies can also be observed by cryo-etch-SEM using pseudodiluted solutions of not only seawater, polymers and silica sols[41−44] but also of neat DESs (Figure 2).[26,35] In our case, cryo-etch-SEM was performed on

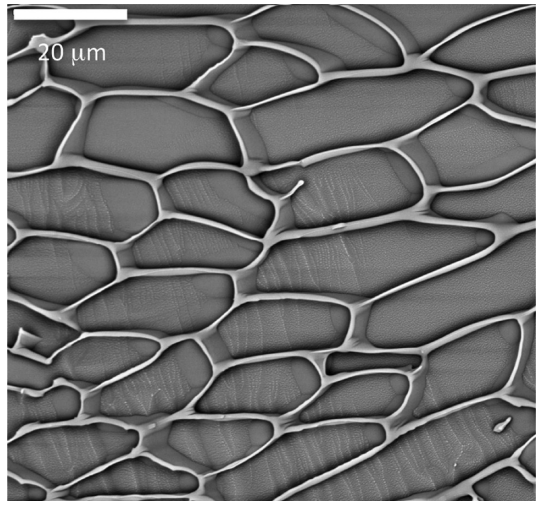

Figure 2. Cryo-etch-SEM micrograph of an aqueous solution of UCCl-DES without EL*b*Rs. Bar is 20 μm.

clear EL*b*R aqueous solutions (also prepared at 4 °C and hence, below the phase transition of EL*b*R) without and with UCCl-DES. In this latter case, the DES components were added in the proper molar ratio but at a high dilution. (See the Experimental Part for further details.) In both cases, the EL*b*R aqueous solutions (maintained at 4 °C) were frozen by simple immersion in subcooled liquid nitrogen (e.g., liquid nitrogen at vacuum pressure). A close inspection to the texture of the fences revealed the differences resulting from the addition of DES components to the EL*b*R aqueous solutions. Thus, EL*b*R aqueous solutions without DES components displayed no further texture than the "fence-like" morphology (Figure 3) in agreement with previous cryo-etch-SEM studies of EL*b*Rs in

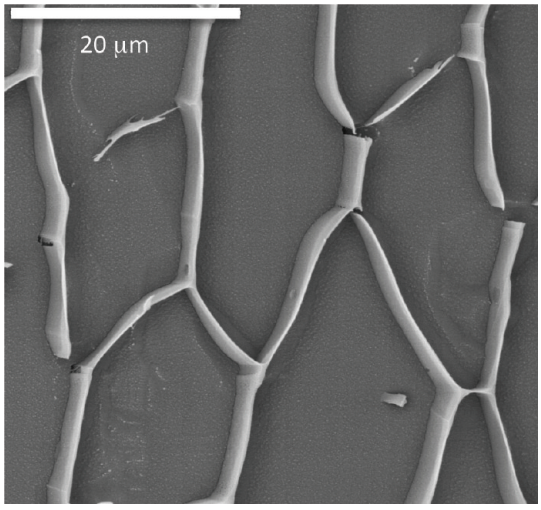

Figure 3. Cryo-etch-SEM micrograph of an aqueous solution of EL*2b*R without UCCl-DES representing a typical "fence-like" morphology. Bar is 20 μm. The cryo-etch-SEM micrograph of an aqueous solution of EL*4b*R without UCCl-DES is not shown because it did not show any significant difference.

the expanded state,[39,40] whereas spherical micellar aggregates (characteristic of the collapsed one[32,33]) could be observed within the "fences" of EL*b*Rs aqueous solutions also containing DES components (Figure 4). Interestingly, micellar structures were also observed by cryo-etch-SEM in EL*b*R aqueous solutions that contained NaCl instead of UCCl-DES (Figure 5). It is generally assumed that in aqueous solutions of EL*b*R the presence of NaCl promotes the stabilization of EL*b*R in both the expanded and the collapsed states of ELP,[45] the former because of the better structured corona of hydrophobic hydration surrounding the nonpolar moieties and the latter due to a typical salting out effect that results in a better organization of the polymer in the collapsed state. Therefore, the formation of EL*b*R micelles after the freeze-drying of both UCCl-DES and NaCl aqueous solutions seems to be favored by the ionic character of the media. Actually, DESs are considered to be part of the ionic liquids family (and hence, molten salts), the ionic strength of which was eventually capable to stabilize the collapsed states of EL*b*Rs by preventing the globular structures from self-fusion processes that typically occur in bare water (Figure 3 and 4a). Nonetheless, it is worth noting that the observation of globular structures was clearer in NaCl than in UCCl-DES because the segregation between globules and the surrounding medium (which is ultimately determining how easy the observation is) is obviously favored for solid (e.g., NaCl) versus liquid (e.g., DES) media.

The occurrence of a salting-out-like process in DESs, in which the ionic strength of the media is favoring the collapsed state of EL*b*Rs, was corroborated when aggregation persisted upon the addition of a certain amount of water (e.g., 24 wt % in Figure 6). The UCCl-DES suspensions of EL*b*Rs only became clear for water contents above 30 wt % (Figure 6) and, even in this case, DSC studies (see DSC plots in Figure 7 and data in Tables 1 and 2) demonstrated that EL*b*R yet remained in the collapsed state. Actually, water contents above 50 wt % were required for recovering of LCST transitions in both EL*2b*R and EL*4b*R.

The persistence of the collapsed state for water contents ranging from 30 to 35 to 50−55 wt % (e.g., clear EL*b*R

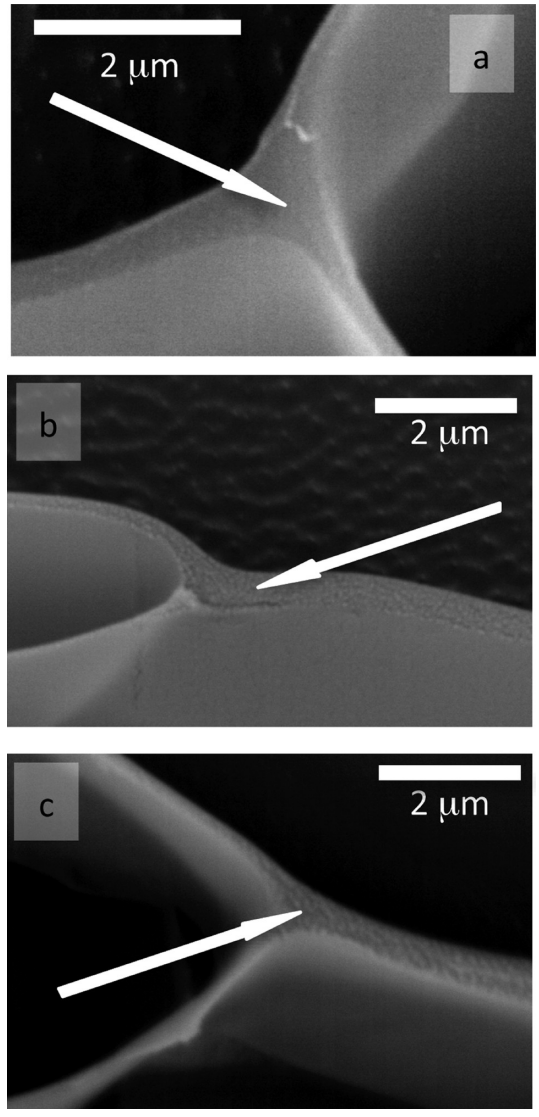

Figure 4. Detail of a cryo-etch-SEM micrograph of an aqueous solution of EL*4b*R without UCCl-DES (a), of an aqueous solution of EL*2b*R that also contains UCCl-DES (b), and of an aqueous solution of EL*4b*R that also contains UCCl-DES (c). In these two latter cases, arrows point to the tiny aggregates of ca. 100 nm that can be observed within the "fence-like structures" formed by UCCl-DES after ice sublimation. Bars are 2 μm. The detail of a cryo-etch-SEM micrograph of an aqueous solution of EL*2b*R without UCCl-DES is not shown because it did not show any significant difference as compared with that of EL*4b*R shown in panel a.

solutions, Figure 6) was confirmed by DLS. Figure 8 shows that water contents of 64 and 54 wt % were required for the observation of the LCST transition from the expanded (low optical density) to the collapsed (high optical density) state in EL*2b*R and EL*4b*R, respectively. Otherwise (e.g., for water contents of 54 wt % in EL*2b*R and 44 wt % in EL*4b*R), the LCST was suppressed and high optical densities were observed along the entire range of temperatures used in the experiment. It is worth noting that the EL*b*R diameters in the collapsed state were below 120 nm in every case as the clear character of all of these solutions anticipated. Nonetheless, it was also observed how these diameters increased along with the decrease in the water content. This feature was in agreement with the above-mentioned formation of larger globular

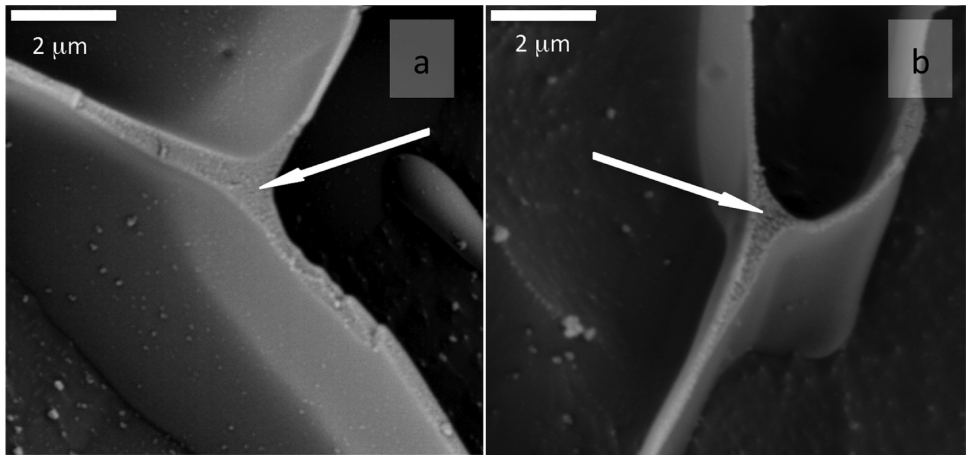

Figure 5. Cryo-etch-SEM micrographs of aqueous solutions of EL*2b*R (a) and EL*4b*R (b) containing 100 mM NaCl. Bars are 2 μm. Arrows point to the tiny aggregates of ca. 100 nm that can be observed within the "fence-like structures" formed by NaCl after ice sublimation.

Figure 6. Picture of different aqueous solutions of UCCl-DES also containing EL*4b*R (from left to right, the water content was 94, 64, 44, 34, 29, and 24 wt %). The EL*4b*R content was always 1 wt %. The picture of different aqueous solutions of UCCl-DES also containing EL*2b*R is not shown because it did not show any significant difference.

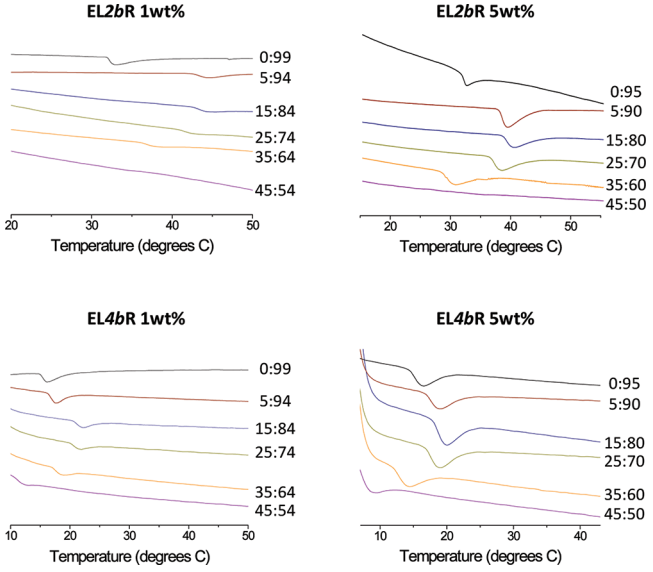

Figure 7. DSC scans of EL*2b*R and EL*4b*R suspended in aqueous solutions of DES. The EL*b*R contents were 1 and 5 wt %. Numbers besides scans represent the DES:water ratio in wt %. Thus, the DES contents (in wt %) ranged from 0 to 45 wt %. DSC scans of EL*b*Rs solutions having 5 wt % were recorded for better observation of the LCSTs. It is worth noting that the absolute value of the LCST (see Tables 1 and 2 for details) slightly depends on the EL*b*Rs content, but the evolution along with the DES content does not.

aggregates under conditions that are favorable for hydrophobic contacts. Whether DLS experiments could be influenced by the particular physical properties of UCCl-DES (e.g., viscosity, refractive index, density, etc.) was disregarded because, at the water contents used in the experiments, differences between UCCl-DES dilutions and bare water were not significant (Table 3).

One may also wonder what (if any) the evolution of neat DES (without EL*b*R) is upon dilution. It is generally assumed that DES dilution promotes the rupture of the original supramolecular complexes that are forming the DES so that for high water contents DES components become individual molecules that are solvated by the aqueous environment. We have recently used ^{1}H NMR spectroscopy to study UCCl-DES rupture along with the water content.[35] Thus, for low water contents (e.g., 15−40 wt %), the chemical shifts of the NMR spectra revealed that water molecules are solvated by UCCl-DES, whereas the opposite situation (i.e., water solvating the individual components of DES) was found for high water contents (70−85 wt %). We also found that transitioning from low to high water contents implies the growth of the water domains that, in a first stage, can be yet solvated by UCCl-DES and, later on, promote the rupture of UCCl-DES into its individual components that are solvated by water molecules.[35] Obviously, the opposite also applies; transitioning from high to low water contents promotes the growing of UCCl-DES domains that, initially (i.e., while they are small enough), are water solvated, but, after further growing, the situation reverts into small water domains solvated by UCCl-DES.

In this stage, it is worth looking again at the DSC curves of EL*b*Rs in water and in aqueous dilutions of UCCl-DES represented in Figure 7. The temperatures of the endothermic peak of EL*2b*R and EL*4b*R in water were 33 and 16 °C, respectively. First addition of DES components (ca. 5−15 wt %) resulted in an increase of in the transition temperature (see the shift of the endothermic peaks in Figure 7, data can be found in Tables 1 and 2) because of the destabilization of the collapsed state.[46] This is actually the same behavior that is observed with the vast majority of proteins in which unfolding is promoted by the strong denaturing character of urea.[47−49] The endothermic peak shifted to lower temperatures upon

dx.doi.org/10.1021/bm300200e | *Biomacromolecules* 2012, 13, 2029−2036

Table 1. Inverse Transition Temperature of Aqueous Solutions of EL*2b*Rs Containing Different DES Contents (from nil to 45 wt %) Obtained from DSC Scans[a]

sample	T_t by DSC (T_t by DLS) (°C)
EL*2b*R 1 wt % - H_2O 99 wt %	33.0
EL*2b*R 1 wt % - DES 5 wt % - H_2O 94 wt %	44.7
EL*2b*R 1 wt % - DES 15 wt % - H_2O 84 wt %	44.3
EL*2b*R 1 wt % - DES 25 wt % - H_2O 74 wt %	42.9
EL*2b*R 1 wt % - DES 35 wt % - H_2O 64 wt %	38.2 (34.0)
EL*2b*R 1 wt % - DES 45 wt % - H_2O 54 wt %	
EL*2b*R 5 wt % - H_2O 95 wt %	32.2
EL*2b*R 5 wt % - DES 5 wt % - H_2O 90 wt %	39.0
EL*2b*R 5 wt % - DES 15 wt % - H_2O 80 wt %	40.0
EL*2b*R 5 wt % - DES 25 wt % - H_2O 70 wt %	38.2
EL*2b*R 5 wt % - DES 35 wt % - H_2O 60 wt %	30.4
EL*2b*R 5 wt % - DES 45 wt % - H_2O 50 wt %	

[a]Inverse transition temperature obtained from DLS experiments is also included for DES contents of 35 wt % (between brackets).

Table 2. Inverse Transition Temperature of Aqueous Solutions of EL*4b*Rs Containing Different DES Contents (from nil to 55 wt %) Obtained from DSC Scans[a]

sample	T_t by DSC (T_t by DLS) (°C)
EL*4b*R 1 wt % - H_2O 99 wt %	16.2
EL*4b*R 1 wt % - DES 5 wt % - H_2O 94 wt %	17.6
EL*4b*R 1 wt % - DES 15 wt % - H_2O 84 wt %	22.2
EL*4b*R 1 wt % - DES 25 wt % - H_2O 74 wt %	22.0
EL*4b*R 1 wt % - DES 35 wt % - H_2O 64 wt %	17.8
EL*4b*R 1 wt % - DES 45 wt % - H_2O 54 wt %	12.6 (9.0)
EL*4b*R 1 wt % - DES 55 wt % - H_2O 44 wt %	
EL*4b*R 5 wt % - H_2O 95 wt %	16.4
EL*4b*R 5 wt % - DES 5 wt % - H_2O 90 wt %	19.0
EL*4b*R 5 wt % - DES 15 wt % - H_2O 80 wt %	20.0
EL*4b*R 5 wt % - DES 25 wt % - H_2O 70 wt %	18.9
EL*4b*R 5 wt % - DES 35 wt % - H_2O 60 wt %	14.3
EL*4b*R 5 wt % - DES 45 wt % - H_2O 50 wt %	8.6
EL*2b*R 5 wt % - DES 50 wt % - H_2O 45 wt %	

[a]Inverse transition temperature obtained from DLS experiments is also included for DES contents of 45 wt % (between brackets).

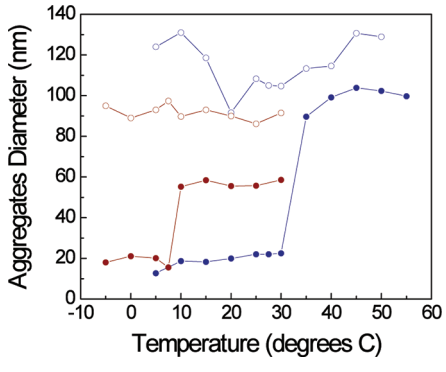

Figure 8. Hydrodynamic diameter of EL*2b*R (blue symbols) and EL*4b*R (red symbols) versus temperature in different aqueous solutions of DES. The water contents in EL*2b*R solutions were 64 (solid symbols) and 54 wt % (open symbol). The water contents in EL*4b*R solutions were 54 (solid symbols) and 44 wt % (open symbol). The EL*b*Rs content was 1 wt %. The heating rate was 1 °C/min.

Table 3. Physical Properties of UCCl-DES and of Its Aqueous Dilutions[a]

UCCl-DES/H_2O (wt %)	viscosity (cP)	density (g/mL)	refractive index
100:0	1108.1	1.192	1.505
95:5	139.2	1.188	1.495
85:15	23.1	1.171	1.483
75:25	6.8	1.150	1.457
65:35	3.1	1.113	1.441
55:45	2.1	1.112	1.420
45:55	1.7	1.090	1.415
35:65	1.5	1.067	1.387
25:75	1.3	1.048	1.372
15:85	1.2	1.026	1.355
5:95	1.1	1.010	1.340
0:100	1	1.000	1.333

[a]Data were taken at 20 °C. The solutions used for DLS experiments are marked in grey.

further addition of DES components (up to intermediate contents ranging from 15 to 35 wt %). According to previous results found by ^{1}H NMR spectroscopy (see above),[35] the formation of urea-choline chloride ion pairs starts within this concentration range. The strong interaction that the DES components themselves establish to form the ion pairs restricts the availability of the individual DES components[50−53] so that whatever their original activity/reactivity was, it tends to decrease or even vanish.[26] In our case, the decrease in the urea denaturing-activity would explain the stabilization of the collapsed state of EL*b*Rs. Nonetheless, the endothermic peak shifting to lower temperatures could also be ascribed to the eventual increase in the ionic strength coming from UCCl-DES formation, as recently demonstrated by calorimetric studies on EL*b*R solutions containing salts (e.g., NaCl).[45] Previous ^{1}H NMR spectroscopy studies also revealed that upon further addition of DES components (ca. 40 wt %) UCCl-DES domains started to prevail over the aqueous ones.[35] For UCCl-DES contents ranging from 45 to 70 wt %, the LCST transitions of EL*2b*R and EL*4b*R were suppressed in the DSC scans over the entire range of temperatures where the LCST typically occurs. This feature was indicative of the preferred stabilization of one of the states that, according to the above-described DLS experiments, was the collapsed one. The prevalence of the collapsed state within this range of UCCl-DES content (e.g., 40−70 wt %) was confirmed when, upon further addition of UCCl-DES (e.g., UCCl-DES contents above 70 wt %), the solution became turbid, resembling the typical aspect of aqueous solutions of EL*b*Rs above the LCST. Figure 9

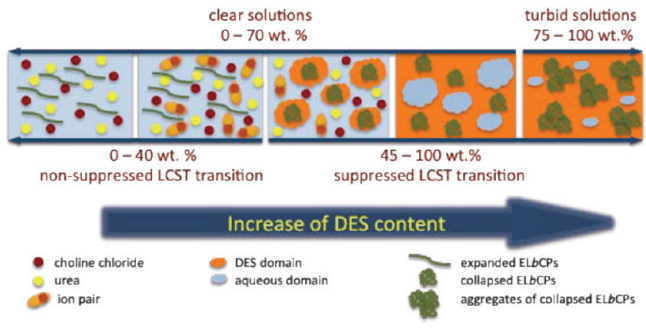

Figure 9. Scheme representing the transition from the expanded to the collapsed state of EL*b*Rs depending on the DES/water ratio.

dx.doi.org/10.1021/bm300200e | *Biomacromolecules* 2012, 13, 2029−2036

provides an idealized representation of the situation of EL*b*Rs (at either the expanded or the collapsed state) and UCCl-DES (in which the components are either dissolved or forming domains) upon the transition from aqueous to poorly or nonhydrated conditions, respectively.

CONCLUSIONS

Summarizing, this manuscript reports on the study of EL*b*Rs suspended in UCCl-DES. Cryo-etch-SEM demonstrated that the preferred conformation of EL*b*R in UCCl-DES is in the collapsed state. DSC and DLS confirmed that UCCl-DES provides a nonhydrated solvent of relatively high ionic strength that favors the stabilization of EL*b*R in the collapsed state. DSC and DLS also revealed that the collapsed state remains stable even after partial hydration (e.g., UCCl-DES aqueous solution with water contents of up to 50−55 wt %). Considering that many nano(bio)technological applications of ELP are related to the occurrence of the LCST transition,[14] the capability to trigger this transition from the expanded to the collapsed state of EL*b*R in UCCl-DES by partial hydration is of interest not only from a fundamental point of view but also from a practical one because it may open novel and interesting fields where EL*b*Rs can be applied.

AUTHOR INFORMATION

Corresponding Author

*E-mail: delmonte@icmm.csic.es.

Notes

The authors declare no competing financial interest.

ACKNOWLEDGMENTS

This work was supported by MICINN (projects MAT2009-10214, MAT2011-25329, MAT2010-15982, MAT2010-15310, ACI2009-0890, and MAT2009-14195-C03-03) and the "Junta de Castilla y León" (VA030A08 and VA034A09). S.N. acknowledges CSIC for a JAE-Pre fellowship.

REFERENCES

(1) Qu, Y.; Payne, S. C.; Apkarian, R. P.; Conticello, V. P. *J. Am. Chem. Soc.* **2000**, *122*, 5014−5015.
(2) Urry, D. W.; Luan, C. H.; Parker, T. M.; Gowda, D. C.; Prasad, K. U.; Reid, M. C.; Safavy, A. *J. Am. Chem. Soc.* **1991**, *113*, 4345−4346.
(3) Meyer, D. E.; Chilkoti, A. *Nat. Biotechnol.* **1999**, *17*, 1112−1115.
(4) Rodríguez-Cabello, J. C.; Reguera, J.; Girotti, A.; Alonso, M.; Testera, A. M. *Prog. Polym. Sci.* **2005**, *30*, 1119−1145.
(5) Cappello, J.; Crissman, J. W.; Crissman, M.; Ferrari, F. A.; Textor, G.; Wallis, O.; Whitledge, J. R.; Zhou, X.; Burman, D.; Aukerman, L.; Stedronsky, E. R. *J. Controlled Release* **1998**, *53*, 105−117.
(6) Spezzacatena, C.; Pepe, A.; Green, L. M.; Sandberg, L. B.; Bochicchio, B.; Tamburro, A. M. *Eur. J. Org. Chem.* **2005**, *8*, 1644−1651.
(7) Nuhn, H.; Klok, H.-A. *Biomacromolecules* **2008**, *9*, 2755−2763.
(8) Winkler, S.; Wilson, D.; Kaplan, D. L. *Biochemistry* **2000**, *39*, 12739−12746.
(9) Urry, D. W. *Angew. Chem., Int. Ed.* **1993**, *32*, 819−841.
(10) Urry, D. W. *J. Phys. Chem.* **1997**, *101*, 11007−11028.
(11) San Biagio, P. L.; Madonia, F.; Trapane, T. L.; Urry, D. W. *Chem. Phys. Lett.* **1988**, *145*, 571−574.
(12) Rodríguez-Cabello, J. C.; Alonso, M.; Pérez, T.; Herguedas, M. M. *Biopolymers* **2000**, *54*, 282−288.
(13) Valiaev, A.; Lim, D. W.; Schmidler, S.; Clark, R. L.; Chilkoti, A.; Zauscher, S. *J. Am. Chem. Soc.* **2008**, *130*, 10939−10946.
(14) Urry, D. W. In *What Sustains Life? Consilient Mechanisms for Protein-Based Machines and Materials*; Springer: Singapore, 2006.
(15) San Biagio, P. L.; Madonia, F.; Trapane, T. L.; Urry, D. W. *Chem. Phys. Lett.* **1988**, *145*, 571−574.
(16) Tamburro, A. M.; Guantieri, V.; Pandolfo, L.; Scopa, A. *Biopolymers* **1990**, *29*, 855−870.
(17) Lelj, F.; Tamburro, A. M.; Villani, V.; Grimaldi, P.; Guantieri, V. *Biopolymers* **1992**, *32*, 159−170.
(18) Schild, H. G.; Tirrell, D. A. *J. Phys. Chem.* **1990**, *94*, 4352−4356.
(19) Rodríguez-Cabello, J. C.; Martín, L.; Alonso, M.; Arias, F. J.; Testera, A. M. *Polymer* **2009**, *50*, 5159−5169.
(20) Xia, F.; Feng, L.; Wang, S.; Sun, T.; Song, W.; Jiang, W.; Jiang, L. *Adv. Mater.* **2006**, *18*, 432−436.
(21) Daamena, W. F.; Veerkampa, J. H.; van Hestb, J. C. M.; van Kuppevelt, T. H. *Biomaterials* **2007**, *28*, 4378−4398.
(22) Woodhouse, K. A.; Klement, P.; Chen, V.; Gorbet, M. B.; Keeley, F. W.; Stahl, R.; Fromstein, J. D.; Bellingham, C. M. *Biomaterials* **2004**, *25*, 4543−4553.
(23) Abbott, A. P.; Capper, G.; Davies, D. L.; Rasheed, R. K.; Tambyrajah, V. *Chem. Commun.* **2003**, 70−71.
(24) Byrne, N.; Angell, C. A. *Chem. Commun.* **2009**, 1046.
(25) Meli, L.; Miao, J.; Dordick, J. S.; Linhardt, R. J. *Green Chem.* **2010**, *12*, 1883−1892.
(26) Gutiérrez, M. C.; Ferrer, M. L.; Yuste, L.; Rojo, F.; del Monte, F. *Angew. Chem., Int. Ed.* **2010**, *49*, 2158−2162.
(27) Perriman, A. W.; Cölfen, H.; Hughes, R. W.; Barrie, C. L.; Mann, S. *Angew. Chem., Int. Ed.* **2009**, *48*, 6242−6246.
(28) Perriman, A. W.; Brogan, A. P. S.; Cölfen, H.; Tsoureas, N.; Owen, G. R.; Mann, S. *Nat. Chem.* **2010**, *2*, 622−626.
(29) Phillips, D. M.; Drummy, L. F.; Conrady, D. G.; Fox, D. M.; Naik, R. R.; Stone, M. O.; Trulove, P. C.; DeLong, H. C.; Mantz, R. A. *J. Am. Chem. Soc.* **2004**, *126*, 14350−14351.
(30) Murugesan, S.; Wiencek, J. M.; Ren, R. X.; Linhardt, R. J. *Carbohydr. Polym.* **2006**, *63*, 268−271.
(31) Vijayaraghavan, R.; Thompson, B. C.; MacFarlane, D. R.; Kumar, R.; Surianarayanan, M.; Aishwarya, S.; Sehgal, P. K. *Chem. Commun.* **2010**, *46*, 294−296.
(32) Ribeiro, A.; Arias, F. J.; Reguera, J.; Alonso, M.; Rodríguez-Cabello, J. C. *Biophys. J.* **2009**, *97*, 312−320.
(33) Martín, L.; Arias, F. J.; Alonso, M.; García-Arévalo, C.; Rodríguez-Cabello, J. C. *Soft Matter* **2010**, *6*, 1121−1124.
(34) Girotti, A.; Reguera, J.; Rodríguez-Cabello, J. C.; Arias, F. J.; Alonso, M.; Matestera, A. *J. Mater. Sci., Mater. Med.* **2004**, *15*, 479−484.
(35) Gutiérrez, M. C.; Ferrer, M. L.; Mateo, C. R.; del Monte, F. *Langmuir* **2009**, *25*, 5509−5515.
(36) Dreher, M. R.; Simnick, A. J.; Fischer, K.; Smith, R. J.; Patel, A.; Schmidt, M.; Chilkoti, A. *J. Am. Chem. Soc.* **2008**, *130*, 687−694.
(37) Kirsop, B. E.; Doyle, A. *Maintenance of Microorganism and Cultured Cells*; Academic Press: London, 1991.
(38) Velikov, V.; Borick, S.; Angell, C. A. *Science* **2001**, *294*, 2335.
(39) McMillan, R. A.; Caran, K. L.; Apkarian, R. P.; Conticello, V. P. *Macromolecules* **1999**, *32*, 9067−9070.
(40) Wright, E. R.; McMillan, R. A.; Cooper, A.; Apkarian, R. P.; Conticello, V. P. *Adv. Funct. Mater.* **2002**, *12*, 149−154.
(41) Menger, F. M.; Zhang, H.; Caran, K. L.; Seredyuk, V. A.; Apkarian, R. P. *J. Am. Chem. Soc.* **2002**, *124*, 1140−1141.
(42) Menger, F. M.; Galloway, A. L.; Chlebowski, M. E.; Apkarian, R. P. *J. Am. Chem. Soc.* **2004**, *126*, 5987−5989.
(43) Ferrer, M. L.; Esquembre, R.; Ortega, I.; Mateo, C. R.; del Monte, F. *Chem. Mater.* **2006**, *18*, 554−559.
(44) Gutiérrez, M. C.; García-Carvajal, Z. Y.; Jobbágy, M.; Yuste, L.; Rojo, F.; Ferrer, M. L.; del Monte, F. *Adv. Funct. Mater.* **2007**, *17*, 3505−3513.
(45) Reguera, J.; Urry, D. W.; Parker, T. M.; McPherson, D. T.; Rodríguez-Cabello, J. C. *Biomacromolecules* **2007**, *8*, 354−358.
(46) Sagle, L. B.; Zhang, Y.; Litosh, V. A.; Chen, X.; Cho, Y.; Cremer, P. S. *J. Am. Chem. Soc.* **2009**, *131*, 9304−9310.
(47) Bennion, B. J.; Daggett, V. *Proc. Natl. Acad. Sci. U.S.A.* **2003**, *100*, 5142−5147.
(48) Schellman, J. A. *Biophys. Chem.* **2002**, *96*, 91−101.

(49) Pace, C. N.; Marshall, H. F. Arch. *Biochem. Biophys.* **1980**, *199*, 270−276.
(50) Carriazo, D.; Gutiérrez, M. C.; Ferrer, M. L.; del Monte, F. *Chem. Mater.* **2010**, *22*, 6146−6152.
(51) Gutiérrez, M. C.; Carriazo, D.; Ania, C.; Parra, J.; Ferrer, M. L.; del Monte, F. *Energy Environ. Sci.* **2011**, *4*, 3535−3544.
(52) Gutiérrez, M. C.; Carriazo, D.; Tamayo, A.; Jiménez, R.; Picó, F.; Rojo, J. M.; Ferrer, M. L.; del Monte, F. *Chem.−Eur. J.* **2011**, *17*, 10533−10537.
(53) Serrano, M. C.; Gutiérrez, M. C.; Ferrer, M. L.; del Monte, F. *Chem. Commun.* **2012**, *48*, 579−581.